Proceedings of the 7th International Conference on Asian and Pacific Coasts (APAC 2013) Bali, Indonesia, September 24-26, 2013

ANALYSIS OF MECHANISM OF SAND DEPOSITION INSIDE A FISHING PORT USING BG MODEL

Y. Ohki [1], T. Uda [2], S. Miyahara [3], M. Serizawa [3], T. San-nami [3] and A. Sumita [1]

ABSTRACT: A large amount of sand deposited in the wave-shelter zone of Ohtsu fishing port located in northern Ibaraki Prefecture, Japan, resulting in a difficulty in navigation at the port entrance. The BG model (a three-dimensional model for predicting beach changes based on Bagnold's concept) was used to solve this problem. Measures against sand deposition inside the port were investigated and the most appropriate measure found for preventing sand deposition was the extension of a jetty by 100 m at the tip of the west breakwater. The applicability of the BG model to such predictions was confirmed.

Keywords: BG model, Ohtsu fishing port, wave-shelter zone, sand deposition, offshore breakwater, numerical simulation

INTRODUCTION

In general, when a long offshore breakwater is extended, the wave field surrounding the offshore breakwater will change, inducing longshore sand transport from the outside to the inside of the wave-shelter zone. As a result, erosion occurs outside the wave-shelter zone in contrast to the sand deposition inside the wave-shelter zone. When such sand deposition occurs in a fishing port or a commercial port, navigation channels fill up; thus, some measures against sand deposition using hard structures are taken, such as the construction of a groin or a jetty. Even though such measures are taken to prevent sand deposition inside the port, they often become insufficient and in most cases, maintenance dredging is often carried out. However, because the same amount of sand dredged from navigation channels is transported again from the nearby coast after the dredging, frequent maintenance dredging is required, and the continuation of such activity triggers the beach erosion of nearby coasts (Serizawa et al., 2007; Uda, 2010). The continuation of this method, therefore, is questionable, and a trade-off issue that the dredging causes beach erosion arises. To fundamentally solve this issue, an effective method of controlling sand deposition into navigation channels by improving the shape of the fishing port breakwaters is required along with the maintenance dredging of the least volume of sand. Although these measures have been taken at many fishing ports or commercial ports in Japan, no general solution has yet been obtained because of the difficulty in the quantitative prediction of bathymetric changes with sufficient accuracy. In this study, Ohtsu fishing port located in northern Ibaraki Prefecture, Japan, was adopted as an example, where a large amount of sand was deposited in the wave-shelter zone after the construction of the offshore breakwater and which showed difficulties in the maintenance of navigation channels. For this purpose, the BG model (a three-dimensional model for predicting beach changes based on Bagnold's concept) (Serizawa et al., 2006) was used.

GENERAL CONDITIONS OF OHTSU FISHING PORT AND NEARBY COASTS

Figure 1(a) shows an aerial photograph taken in May 2009 around Ohtsu fishing port and the nearby coasts including Point Tenpisan located 3.5 km south of the fishing port in Ibaraki Prefecture, and Fig. 1(b) shows an enlarged aerial photograph of the rectangular area in Fig. 1(a). Ohtsu fishing port is located south of the Izura rocky coast composed of unconsolidated layers. The south breakwater of 802 m length and the south breakwater (offshore) of 369 m length, with an opening of 50 m between them, were constructed, as shown in Fig. 1(b).

In the wave-shelter zone of the above breakwaters, coarse sand with a median diameter of 0.6 mm, which was sampled in 2009 at P on the shoreline, as shown in Fig. 1(b), deposited to form a triangular sandy beach. In contrast, the Kamiokakami coast immediately south of the fishing port was severely eroded with the seawall being exposed to waves (Uda, 2010). Also, the Isohara coast located further south was protected using five

[1] Laboratory of Aquatic Science Consultant Co., Ltd., 1-14-1 Kami-ikedai, Ota, Tokyo 145-0064, JAPAN
[2] Public Works Research Center, 1-6-4 Taito, Taito, Tokyo 110-0016, JAPAN
[3] Coastal Engineering Laboratory Co., Ltd., 1-22-301 Wakaba, Shinjuku, Tokyo 160-0011, JAPAN

(a) Ohtsu fishing port – Point Tenpisan (May 2009)

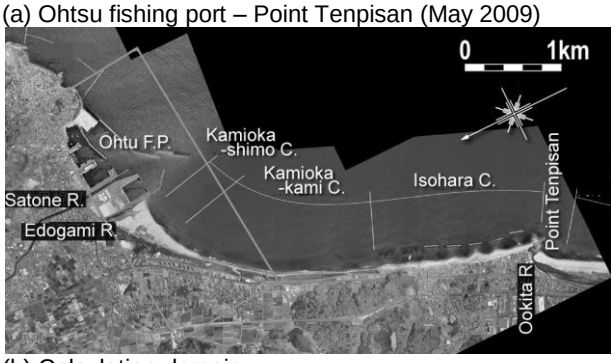

(b) Calculation domain

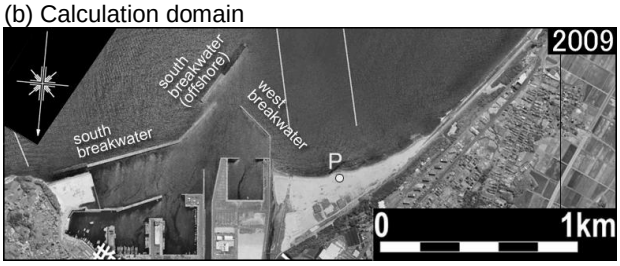

Fig. 1 Aerial photograph around Ohtsu fishing port in northern Ibaraki Prefecture and calculation domain.

detached breakwaters because of the erosion. In contrast, the shoreline next to the west breakwater of the fishing port advanced by approximately 400 m and some of the sand was transported into the navigation channel of the fishing port. The sand deposition near the port was considered to be triggered by the northward longshore sand transport induced by the formation of the wave-shelter zone by the south breakwater. We adopted the rectangular area shown in Fig. 1(b) as the calculation domain.

NUMERICAL MODEL

The BG model proposed by Serizawa et al. (2006) was applied to predict the beach changes. We used Cartesian coordinates (x, y), in which the x- and y-axes were taken in the cross-shore (shoreward positive) and longshore directions, respectively, and considered that the seabed elevation Z (x, y, t) with reference to the still water level is a variable to be solved, where t is the time. The beach changes were assumed to occur between the depth of closure h_c and the berm height h_R. For the sand transport equation, Eq. (1) expressed in terms of the wave energy at the breaking point was used with the variables given by Eqs. (2) - (6). Here, Eq. (1) was improved from the original equation proposed by Serizawa et al. (2006) by including the coefficients of both longshore and cross-shore sand transports, and an additional term given by Ozasa and Brampton (1980) was incorporated into Eq. 1(b) to evaluate the longshore sand transport owing to the effect of the longshore gradient of the breaker height.

$$q_x=\frac{G_x}{\tan\beta_c}[\tan\beta_c\cos\theta_w-\partial Z/\partial x] \qquad (-h_c\le Z\le h_R) \quad (1a)$$

$$q_y=\frac{G_y}{\tan\beta_c}\left[\tan\beta_c\left(\sin\theta_w-\frac{1}{\tan\overline{\beta}}\frac{K_2}{K_y}\frac{\partial H_b}{\partial y}\right)-\partial Z/\partial y\right] \qquad (-h_c\le Z\le h_R) \quad (1b)$$

$$G_x=K_xG,\ G_y=K_yG \quad (2)$$

$$G=C_0\varepsilon(Z)(EC_g)_b\cos^2\alpha_b\tan\beta_c \quad (3)$$

$$C_0=\frac{1}{(\rho_s-\rho)g(1-p)} \quad (4)$$

$$\int_{-h_c}^{h_R}\varepsilon(Z)dZ=1 \quad (5)$$

$$\varepsilon(Z)=\begin{cases}=\dfrac{1}{h_c+h_R} & (-h_c\le Z\le h_R)\\ =0 & (Z<-h_c,\ h_R<Z)\end{cases} \quad (6)$$

$$(EC_g)_b=C_1(H_b)^{\frac{5}{2}} \quad (7a)$$

$$C_1=\frac{\rho g}{k_1}\sqrt{g/\gamma} \qquad \left(k_1=(4.004)^2,\ \gamma=0.8\right) \quad (7b)$$

Here, q_x and q_y are the x- and y-components of sand transport flux, θ_w is the wave angle measured counterclockwise with respect to the direction of the x-axis, $(EC_g)_b$ is the energy flux at the breaking point, α_b is the breaker angle, and $\tan\beta_c$ is the equilibrium slope of sand such that cross-shore sand transport becomes 0 when waves are incident normal to the shoreline. K_x and K_y are the coefficients of cross-shore and longshore sand transports, respectively, K_2 is the coefficient of the term given by Ozasa and Brampton (1980), H_b is the breaker height, and $\tan\overline{\beta}$ is the seabed slope at the breaker point. In this study, we assumed $\tan\overline{\beta}=\tan\beta_c$. C_0 is the coefficient transforming the immersed weight expression into a volumetric expression ($C_0=1/\{(\rho_s-\rho)g(1-p)\}$, where ρ is the density of seawater, ρ_s is the specific gravity of sand particles, p is the porosity of sand, and g is the acceleration due to gravity).

$\varepsilon(Z)$ is the depth distribution of the intensity of longshore sand transport, and a uniform distribution as in Eq. (6) is assumed for the integral of $\varepsilon(Z)$ over the depth zone between $-h_c$ and h_R to be equal to 1. Equation 7(a) shows the relationship between the energy flux at the breaking point and the breaker height, assuming the linear shallow water wave theory. γ is the ratio of the breaker height relative to the water depth. In addition, k_1 = $(4.004)^2$ in Eq. (7b) is a constant in the relationship between the wave energy E and the significant wave

height when the probability of the wave height of irregular waves is assumed to be given by the Rayleigh distribution (Horikawa, 1988). The beach changes were calculated using the continuity equation of sand along with the sand transport equations.

The calculation domain was discretized in 2-D elements with widths of $\otimes x$ and $\otimes y$. The calculation points of the seabed elevation Z and sand transport rate $\vec{q}=(q_x, q_y)$ were distributed using staggered meshes with a half mesh interval, and Eqs. (1) - (7) were solved by the explicit finite difference method. Calculations were recurrently carried out. For the boundary conditions, sand transport was set to be 0 at the solid boundary.

The wave field necessary for the calculation of the beach changes was calculated using the angular spreading method for irregular waves (Sakai et al., 2006; Uda, 2010). In the area without the wave diffraction effect of the structures, the incident wave height H_I was assumed to be approximately equal to the breaker height H_b, and we assumed the direction of incident waves θ_I to be for the wave direction at a point, θ_w. In addition, the breaker angle at each point θ_b was assumed to be the angle between the wave direction at each point, θ_w and the direction (shoreward positive) normal to the contours, θ_n.

In the wave-shelter zone of the offshore breakwaters, the distribution of the wave diffraction coefficient K_d and the direction of diffracted waves θ_d were calculated using the angular spreading method, and the wave height H_b under the conditions without the offshore breakwaters was reduced by multiplying K_d. The wave direction at any point was assumed to be equal to θ_d. In estimating the intensity of sand transport near the berm top and at the depth of closure, the intensity of sand transport was linearly reduced to 0 near the berm height or the depth of closure to prevent sand from being deposited in the zone higher than the berm height and the beach from being eroded in the zone deeper than the depth of closure, as described by Uda et al. (2013).

CALCULATION CONDITIONS

Two types of calculation were carried out: the reproduction of the present conditions and the prediction of the beach changes. In the reproduction calculation, the beach changes associated with the extension of south breakwater (offshore) between 1998 and 2009 were reproduced and the applicability of the model was validated by comparing the measured and calculated shoreline changes. For this purpose, waves were incident to the modeled initial bathymetry with parallel contours for a sufficiently long time of 30 years, and a stable initial bathymetry before the construction of the offshore breakwaters in 1998 was obtained. The beach changes

Table 1 Calculation conditions.

Study area	Ohtsu fishing port and nearby coasts
Calculation methods	BG model for predicting beach changes originally proposed by Serizawa et al. (2006) and then improved Angular spreading method for irregular waves (Sakai et al., 2006)
Period of reproduction calculation	Between 1998 and 2009
Prediction calculation	Duration of prediction: 10 years Case 1: No measures taken Case 2: Jetty construction at the entrance of channel Case 3: Leave as it was after dredging of sand deposited inside port Case 4: Jetty construction of a jetty at the entrance of channel with removal of sand Case 5: Case 3 + action of extremely high waves for 10 days Case 6: Case 4 + action of extremely high waves for 10 days
Initial bathymetry	Reproduction calculation: Stable bathymetry in 1998 when uniform slope of 1/30 was given as initial bathymetry. Prediction: reproduced bathymetry in 2009
Wave conditions	Energy-mean waves: H_I = 1.5 m, T = 8 s, wave direction of S50°E and S_{max} = 10 Extremely high waves: H_I = 5 m and S_{max} = 10
Sea level	Mean sea level
Berm height	h_R = 2.5 m
Depth of closure	h_c = 9 m
Equilibrium slope	$\tan\beta_c$ = 1/30 (1/100 for depth zone between -7 and -9 m)
Depth distribution of sand transport	Uniform
Angle of repose slope	$\tan\beta_g$ = 1/2
Coefficients of sand transport	Coefficient of longshore sand transport K_x = 0.08 Coefficient of cross-shore sand transport K_y/K_x =1.0 Coefficient of Ozasa and Brampton (1980) term $K_2 = 1.62K_y$
Mesh size	$\otimes x$ = 20 m
Time intervals	$\otimes t$ = 5 hr/step and $\otimes t$ = 1 hr/step in Cases 5 and 6
Duration of calculation	10 years
Boundary conditions	Right, left and landward ends: q = 0 Seaward boundary: dq_x/dx = 0
Other remarks	Wave transmission coefficient of detached breakwater: K_t = 0.6

until 2009 were predicted given this bathymetry as the initial bathymetry.

In the prediction of beach changes, the bathymetry in 2019 was predicted and six cases of calculations were carried out. In Case 1, no measures were taken. In Case 2, a jetty was constructed at the entrance of the port to prevent sand movement into the navigation channel. In Case 3, sand deposited inside the port was first removed and then left as it was without any further measures. In Case 4, a jetty was constructed at the entrance of the port to prevent sand movement into the navigation channel after the removal of deposited sand. The facilities in Cases 1 and 2 have the same shape as those in Cases 3 and 4. The difference is in whether the navigation channel is left as it was or the deposited sand was removed. In Cases 5 and 6, the effect of extremely high waves was calculated against Cases 3 and 4, respectively, assuming that the duration of storm waves was 10 days.

For the wave conditions, the energy-mean wave height of H_I = 1.5 m obtained from the observation data between 1984 and 1994 measured 6 km offshore of Point Tenpisan (Shidai et al., 1997) was used. Although the prevailing wave direction measured by Higuchi et al. (1997) and Shidai et al. (1997) was ESE, in this calculation, the wave direction was determined to be S50°E by trial and error calculation, in which best fit calculation results were obtained against the measured shoreline.

The construction of the south breakwater (offshore) was started in 1989. First, it was extended by 250 m length between 1989 and 1995 and the entire length had become 369 m by 2003 owing to further extension by 120 m between 1998 and 2003. Because the south breakwater (offshore) was gradually extended with time, the bathymetries in 1998 and 2009 were reproduced. The initial bathymetry used for the reproduction calculation was the bathymetry that reached a stable form against wave action after the arrangement of breakwaters in 1998. Although the south breakwater (offshore) had been extended to two-thirds of the entire length of 369 m until 1998, the effect of the south breakwater on the beach changes was partially observed without reaching a stable condition. Therefore, half of the entire length of 185 m, which is shorter than the real length of 250 m, was given as the breakwater length.

In the calculation of the stable bathymetry in 1998, a flat solid bed with the depth of closure of this coast (h_c = 9 m) was assumed, and a sandy beach with a slope of 1/30 was considered on this flat bed in the zone shallower than -7 m (1/100 in a zone between -7 and -9 m). The initial shoreline was determined so as to fit the shoreline configuration in 1998 by the trial and error method. Under this modeled initial bathymetry, waves were incident for a sufficiently long time of 30 years and a stable initial bathymetry corresponding to the offshore breakwaters (half of the entire length) constructed until 1998 was calculated. The directional spreading parameter S_{max} was assumed to be 10 for wind waves, so that the strong wave-sheltering effect due to the offshore breakwaters was expected. The berm height h_R was assumed to be 2.5 m on the basis of the measurement, and the equilibrium slope was assumed to be 1/30 in the zone shallower than -7 m and 1/100 in the depth zone between -7 and -9 m from the measured longitudinal profile (Uda, 1997).

In the prediction of the beach changes, the reproduced bathymetry in 2009 was regarded as the initial bathymetry. As a measure of preventing sand from depositing in the fishing port, a jetty of 100 m length was assumed to be built at the tip of the west breakwater. The prediction period was set to be 10 years, and additional cases in which extremely high waves were incident to the beaches apart from the incidence of the energy-mean waves were also investigated, setting a relatively short duration time for the typhoon waves. The height of such extremely high waves was assumed to be H_I = 5 m with the wave direction from SSE. This corresponds to a 0.2 % probability of extremely high waves being measured at the wave observatory offshore of Point Tenpisan (Shidai et al., 1997). The wave direction of SSE was adopted as the wave direction from which sand transport toward the wave-shelter zone became most dominant. In this case, S_{max} was also assumed to be 10. The duration of wave action was 10 days considering the accumulation of waves with a probability of once in a year.

RESULTS

Reproduction

Although the numerical calculation was carried out using Cartesian coordinates (x, y), in which the x- and y-axes are taken in the cross-shore (shoreward positive) and longshore directions, respectively, the results are easy to understand when the x-axis is replaced with the y-axis and we adopt the cross-shore coordinate being seaward positive. Therefore, we define Cartesian coordinates (X, Y), in which the X- and Y-axes are taken in the longshore and cross-shore (seaward-positive) directions. Figure 2 shows the results of the reproduction calculation using these coordinates (X, Y). Since a wave-shelter zone due to the south breakwater had already formed by 1998, sand was transported northward, resulting in a shoreline advance in the vicinity of the fishing port. Then, beach changes up to 2009 after the construction of the south breakwater (offshore) were

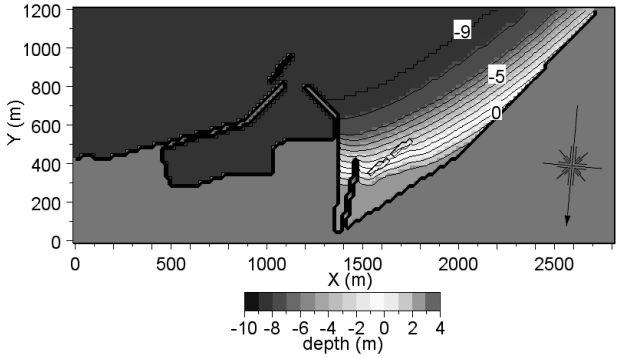

Fig. 2 Calculated bathymetry in 1998 to be used for initial bathymetry in prediction.

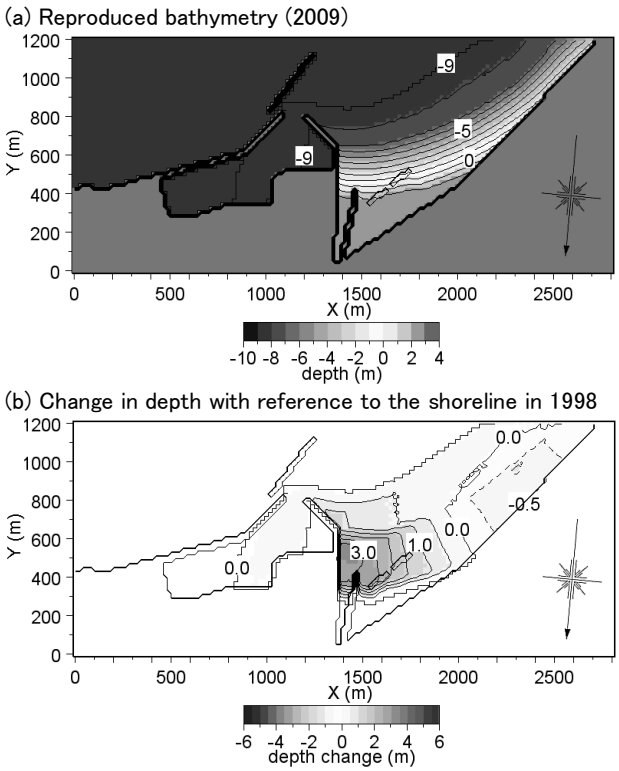

Fig. 3 Reproduced bathymetry in 2009 and bathymetric changes with reference to that in 1998.

calculated, given the bathymetry shown in Fig. 2 as the initial bathymetry. Figure 3 shows the bathymetry in 2009 and the depth changes with reference to that in 1998. The south breakwater (offshore) was extended by 185 m compared with that in 1998, resulting in the southward expansion of the wave-shelter zone and sand deposition inside the wave-shelter zone.

Figure 4 shows the calculated shoreline configuration superimposed on the aerial photographs in 1996 close to the prediction years of 1998 and 2009. The measured and predicted shorelines are in good agreement. It is also realized that the shoreline advanced by 100 m along the west breakwater between 1998 and 2009, and that the Edogami River mouth next to the west breakwater was completely enclosed by sand deposition.

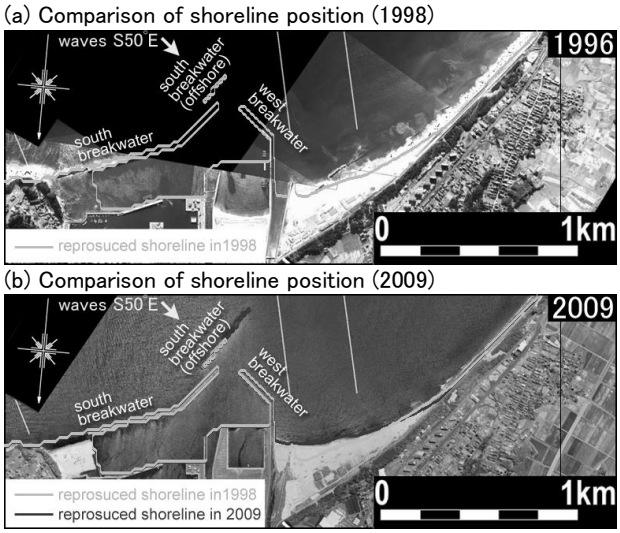

Fig. 4 Measured and calculated shoreline configurations in 1998 and 2009.

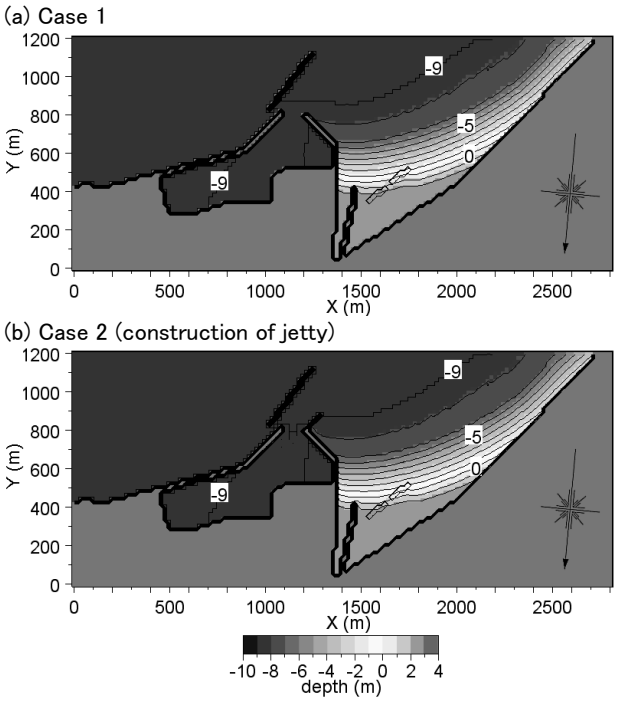

Fig. 5 Predicted bathymetries in Case 1 without any measures taken and Case 2 with jetty construction.

Cases 1 and 2

Figures 5 and 6 show the bathymetries of Cases 1 (no measure) and 2 (jetty construction) in 2019 and their bathymetric changes with reference to the bathymetry in 2009. In Case 1 with no measure taken, sand was not only deposited in the sand accumulation zone south of the west breakwater but also was transported deep inside the fishing port through the navigation channel at the tip of the west breakwater. In this case, note that no sand was transported along immediately inside of the west breakwater but along the south breakwater (offshore). This means that, without any measure, sand deposition

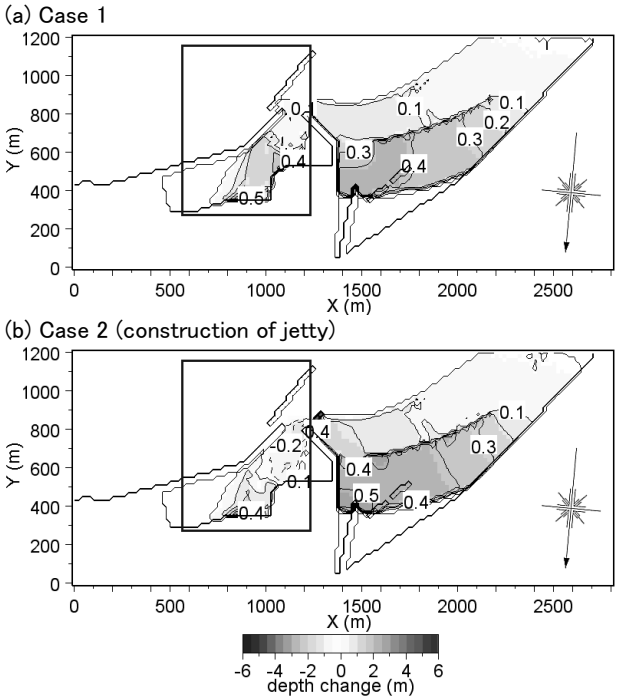

Fig. 6 Bathymetric changes in Case 1 without any measures taken and Case 2 with jetty construction with reference to that in 2009.

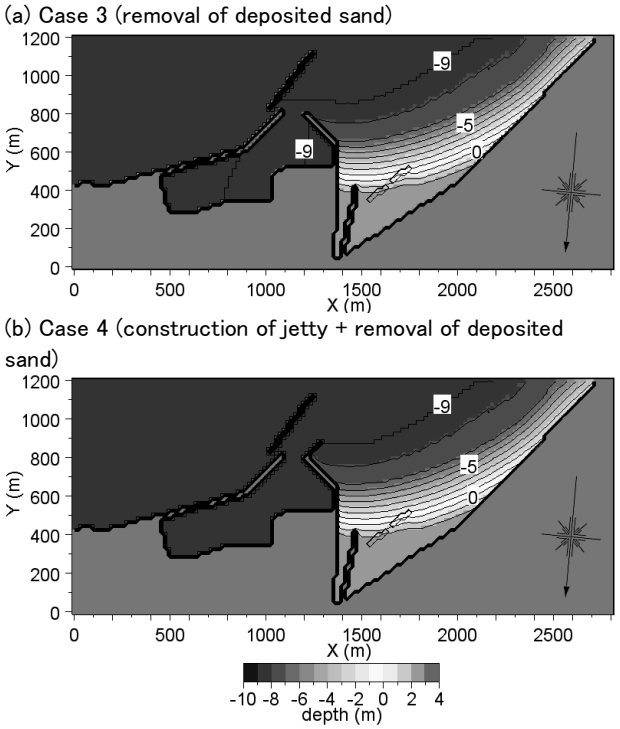

Fig. 7 Bathymetries in Case 3 without any measures taken and Case 4 with jetty construction after removal of sand deposited inside fishing port.

Table 2 Volumes of sand deposited inside the fishing port.

	Initial volume of sand	Increment of volume of sand	Total volume of sand deposited
m^3	V_0	ΔV	$V=V_0+\Delta V$
Reproduction calculation	0	11500	11500
Case 1	11500	21600	33100
Case 2	11500	0	11500
Case 3	0	21600	21600
Case 4	0	0	0
Case 5	21600	26400	48000
Case 6	0	7400	7400

will further continue.

In Case 2 in which a jetty was constructed as a measure, although the effect seems to be small only from Fig. 5, it is found from Fig. 6 that sand transport from the south part of the west breakwater toward the fishing port was blocked by the L-shaped jetty. Although sand deposition deep inside the fishing port can be observed, this was transported from the entrance channel between the south breakwater (offshore) and the west breakwater. The volume of sand deposited in a rectangular area including the sand accumulation zone, as shown in Fig. 6, was 1.15×10^4 m^3 until 2009, but the volume of deposited sand further increased by 2.16×10^4 m^3 in Case 1 with no measures taken (Table 2). In total, 3.31×10^4 m^3 of sand was deposited in Case 1. In contrast, in Case 2 with the construction of a jetty, no further sand accumulation occurred, while keeping the same total volume of sand accumulation of 1.15×10^4 m^3. Thus, it was found that the jetty extension in the direction normal to the existing west breakwater was effective as a measure preventing sand deposition inside the fishing port.

Cases 3 and 4

In Cases 1 and 2, the effect of the jetty construction was investigated while the sand deposited in the port was left as it was. It was, however, difficult to separately understand whether sand deposited at the entrance of the port was transported deep inside the port or sand was transported inside the port after turning around the tip of the jetty. As a result, the effect of the jetty construction became obscure. In Cases 3 and 4, therefore, calculations were carried out, with the bathymetry after the deposited sand was removed as the initial bathymetry.

Figure 7 shows the predicted bathymetries in 2019 in Cases 3 (no measures) and 4 (jetty construction), and Fig. 8 shows their bathymetric changes since 2009 with reference to the bathymetry after the deposited sand was removed. Although the difference between the bathymetries shown in Fig. 7 seems small, a marked difference can be seen in the bathymetric changes in Fig. 8. In Case 3 with no measures taken, sand was transported into the port through the navigation channel

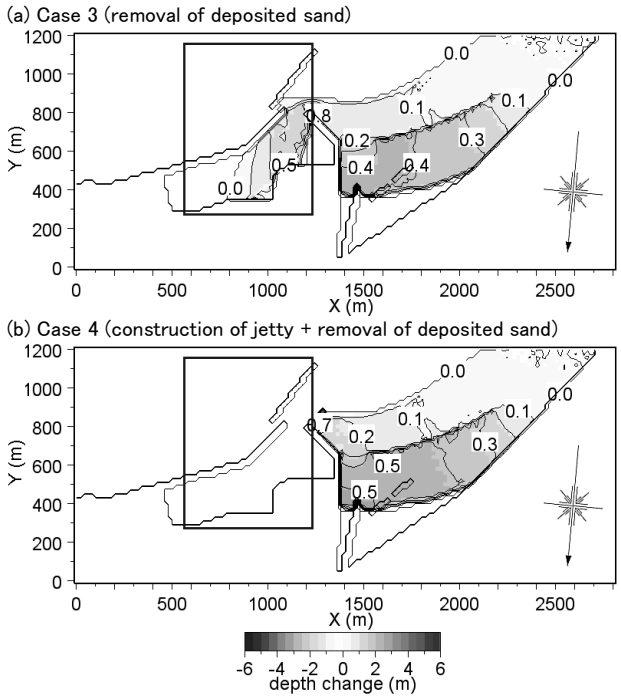

Fig. 8 Bathymetric changes in Case 3 without any measures taken and Case 4 with jetty construction after removal of sand deposited inside fishing port.

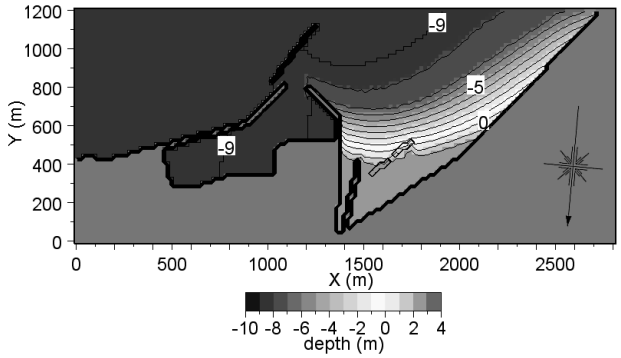

Fig. 9 Bathymetry when extremely high waves act on bathymetry in Case 3 with no measures taken (Case 5).

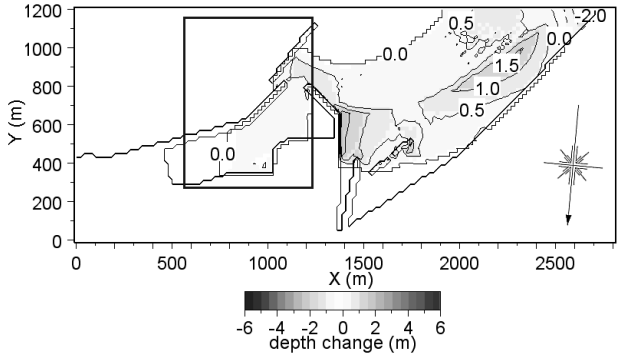

Fig. 10 Bathymetric changes when extremely high waves act on bathymetry in Case 3 with no measures taken (Case 5).

at the tip of the west breakwater, whereas the intrusion of sand into the navigation channel and the port was

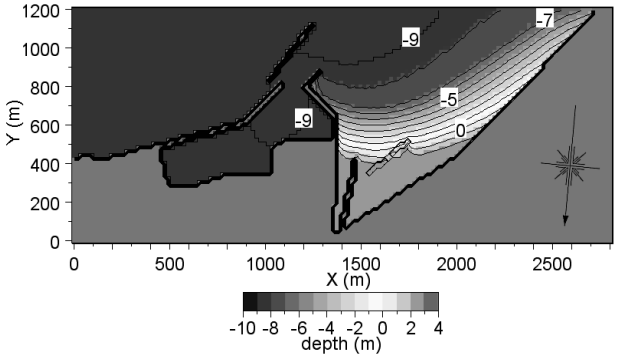

Fig. 11 Bathymetry when extremely high waves act on bathymetry in Case 4 with jetty construction (Case 6).

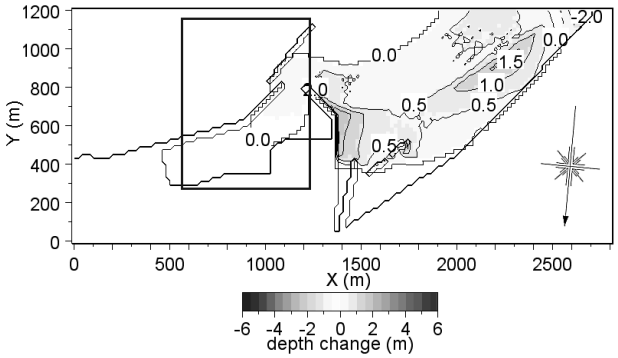

Fig. 12 Bathymetric changes when extremely high waves act on bathymetry in Case 4 with jetty construction (Case 6).

markedly prevented by the jetty construction in Case 4. When calculating the volume of sand deposited in the rectangular area shown in Fig. 8, 2.16×10^4 m^3 of sand was newly deposited in Case 3 after 1.15×10^4 m^3 of sand was removed from the beginning. On the other hand, in Case 4 after a new jetty was constructed along with the removal of 1.15×10^4 m^3 of sand, the volume of sand deposited was nil, suggesting the effectiveness of the construction of a jetty.

Cases 5 and 6

Figures 9 and 10 show the bathymetry in Case 5 in which extremely high waves were incident to the resulting bathymetry in Case 3 for 10 days and the bathymetric changes with reference to the bathymetry before the action of extremely high waves, respectively. Calculating the volume of sand deposited in the rectangular area as shown in Fig. 10, 2.64×10^4 m^3 of sand further accumulated in Case 5 in which extremely high waves were incident under the same condition in Case 3, reaching a total sand volume of 4.8×10^4 m^3. Similarly, Figs. 11 and 12 show the bathymetry in Case 6 in which extremely high waves were incident to the resulting bathymetry in Case 4 (jetty construction) for 10 days and the bathymetric changes with reference to the bathymetry before the action of extremely high waves,

respectively. In Case 6, the volume of sand deposited inside the port markedly decreased. Comparing Case 6 with the jetty construction with Case 5 with no measures taken, sand deposition inside the fishing port was markedly prevented, even though extremely high waves were incident to the beach. Calculating the volume of sand deposited in the rectangular area, as shown in Fig. 12, in Case 6 in which extremely high waves were incident to the condition of Case 5, the volume reached 0.74×10^4 m^3, which was significantly reduced compared with 2.64×10^4 m^3 in Case 5.

CONCLUSION

A large amount of sand was deposited in the wave-shelter zone of Ohtsu fishing port associated with the extension of the offshore breakwaters, causing difficulties in the maintenance of the navigation channel. The BG model (a 3-D model for predicting beach changes based on Bagnold's concept) was used to predict beach changes under the conditions with/without measures taken, taking this fishing port as an example. In the validation of the model, the predicted and measured shoreline configurations were compared and found to be in good agreement. It was also found that sand deposition will further continue in the case without any measures taken, and that the extension of a jetty by 100 m in the direction normal to the west breakwater was very effective as a measure of mitigating sand deposition inside the fishing port. Finally, the effectiveness of the application of the BG model to these predictions was confirmed.

REFERENCES

Higuchi, T., Nishizawa, M., Kawamura, T. and Uda, T. 1997. Changes in the nearshore topography around the cape resulting from intermittent movement of littoral drift, Proc. Coastal Eng., JSCE, Vol. 44, pp. 626-630. (in Japanese)

Horikawa, K. ed. 1988. *Nearshore Dynamics and Coastal Processes*, University of Tokyo Press, Tokyo, p. 522.

Ozasa, H. and Brampton, A. H. 1980. Model for predicting the shoreline evolution of beaches backed by seawalls, Coastal Eng., Vol. 4, pp. 47-64.

Sakai, K., Uda, T., Serizawa, M., Kumada, T. and Kanda, Y. 2006. Model for predicting three-dimensional sea bottom topography of statically stable beach, Proc. 30th ICCE, pp. 3184-3196.

Serizawa, M., Uda, T., San-nami, T. and Furuike, K. 2006. Three-dimensional model for predicting beach changes based on Bagnold's concept, Proc. 30th ICCE, pp. 3155-3167.

Serizawa, M., Uda, T., San-nami, T., Furuike, K. and Ishikawa, T. 2007. BG-model predicting three-dimensional beach changes based on Bagnold's concept and applications, Asian and Pacific Coasts 2007, Proc. 4th International Conf., pp. 1165-1179.

Shidai, A., Kawamura, T., Tanaka, M., Okuma, Y. and Uda, T. 1997. Field investigation of beach changes between Ohtsu fishing port and Point Takado in Ibaraki Prefecture, Proc. Coastal Eng., JSCE, Vol. 44, pp. 656-660. (in Japanese)

Uda, T. 1997. *Beach Erosion in Japan*, Sankaido Shuppan, Tokyo, p. 442. (in Japanese)

Uda, T. 2010. *Japan's Beach Erosion - Reality and Future Measures*, World Scientific, p. 418.

Uda, T., Gibo, M., Ishikawa, T, Miyahara, S., San-nami, T. And Serizawa, M. 2013. Change in carbonate beach triggered by construction of a bridge on Irabu Island and its simulation using BG model, Asian and Pacific Coasts 2013, Proc. 7th International Conf. (in press)